Screen Printed Perovskite Solar Cells with a Mesoscopic Scaffold and Carbon Electrode without a Hole Transport Layer Fabricated and Characterized in an Undergraduate Research Laboratory

Adam Dvorak Physics & Astronomy Pomona College Claremont, USA adam.dvorak@pomona.edu

Bry Hyunjin Hong Physics & Astronomy Pomona College Claremont, USA hyunjin.hong@pomona.edu

Phuong Nguyen Computer Science Pomona College Claremont, USA Phuong.Nguyen@pomona.edu

David M. Tanenbaum Physics & Astronomy Pomona College Claremont, USA David.Tanenbaum@pomona.edu

Abstract—We fabricate and characterize perovskite solar cells with a mesoscopic scaffold of metal oxides and carbon nanomaterials that are screen printed and infiltrated with a perovskite precursor solution. We demonstrate reproducible results with hundreds of samples produced and measured in an undergraduate research laboratory. We combine imaging and analysis techniques with long term light soaking to report the stability of our cells and modules over time and to investigate the degradation mechanisms. Our cells have negligible hysteresis, efficiencies over 12%, and high current densities and open circuit voltages. Fill factors limit our cell performance. (Abstract)

Keywords—perovskite, screen printing, carbon, mesoporous, scaffold, undergraduate research (key words)

I. INTRODUCTION

Solar cells are among the most promising technologies available to sustainably produce the renewable energy needed to continue societal advancement and limit global climate change. While research in solar technologies has been active for over 60 years, the impending global warming scenarios have made this a crucial issue for the current generation of undergraduate (any younger) students who anticipate an environmental catastrophe within their lifetime. These students are highly motivated to advance research in this area and with guidance can do this beginning in their first year in college, enabling them to have longer and more fruitful research experiences. The first three authors on this paper all began their research in the Tanenbaum Laboratory during their first year at Pomona College.

Perovskite based solar cells have demonstrated performance comparable to existing silicon technologies with potential for significant improvements and fast embedded energy payback times. Any solar technology must balance the key parameters of efficiency, cost, and lifetime to be viable for large scale implementation. Solution based processing of thin film materials enables a wide variety of fabrication techniques that enable low-cost large-scale fabrication.

Structural scaffolds made from mesoporous layers of TiO₂, ZrO₂, and Carbon can be printed and infiltrated with perovskite precursor solutions to form efficient and stable solar cells and modules as first demonstrated by the Hongwei Han research group [1]. These types of devices have been demonstrated to be compatible with a variety of scalable processing techniques with potential for very low manufacturing costs. In addition, the perovskite infiltrated Carbon back electrode is low-cost, highly stable, and protects the sensitive photoactive layers from chemical degradation. Another benefit of the Carbon electrode is that it effectively replaces not only the gold electrodes commonly used on perovskite solar cells, but also eliminates the need for exotic hole transport layers like spiro-OMeTAD.

II. METHODS

A. Fabrication steps

We start fabrication of perovskite solar cells on 10 cm x 15 cm substrates of FTO-coated glass. After spraying a compact TiO₂ hole blocking layer and laser scribing isolation lines, we screen print mesoporous layers of TiO2 (electron transport layer), ZrO₂ (insulating layer), and carbon (back electrode) inks and bake on a hot plate in quick succession up to 500°C. We print 36 cells onto a single glass substrate, each with an active area of 0.49 cm². Typical layer thickness are 0.5 µm, 1.0 µm and 10 µm for the TiO₂, ZrO₂, and carbon layers respectively as measured via cross sectional scanning electron microscopy of completed devices.

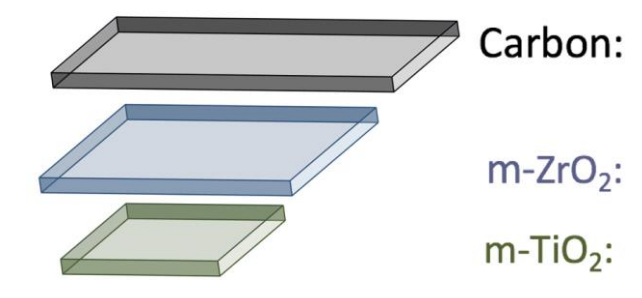


Fig. 1. The m-TiO₂ layer is 7 mm x 7 mm, the m-ZrO2 layer is 9 mm x 11 mm, and the Carbon layer is 7 mm x 14 mm. The upper 2 layers span the laser scribed isolation line which can be clearly seen running across the device in Fig. 4.

This work is supported by a Hirsch Grant at Pomona College and the MRI program from the National Science Foundation.

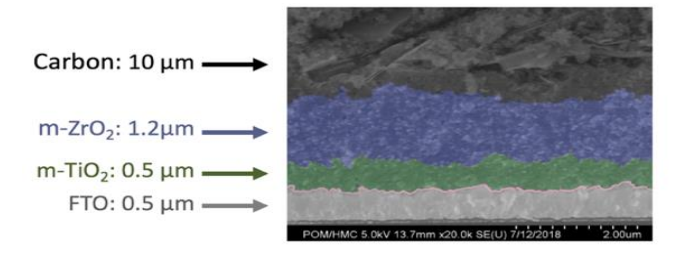


Fig. 2. Cross-section SEM image of our cell structure.

For our perovskite precursor, we combine 5-AVAI, MAI, and PbI₂ with y-butyrolactone (GBL) [2] in a nitrogen glovebox to limit possible lead contamination. The solution is then heated and stirred on a hot plate overnight, or until there are no solids. We have found perovskite precursor has a tendency to overflow the carbon and ZrO₂ layers, leaking current by shorting out the cell. To prevent this, we take a few precautions. First, we only use the minimum precursor necessary (around 1.5-2µL), so there is less solution that can overflow. Second, we laser-cut a stencil mask on a paper sticky note roll that surrounds each cell, enabling the paper to absorb excess perovskite. Third, if necessary, we use a cotton swab and GBL to clear any visible perovskite beyond the scaffold. We infiltrate the perovskite precursor with the substrate at a slight tilt from the horizontal (about 8°) using gravity in addition to capillary forces to help elongate the infiltration of the rectangular (7 mm x 14 mm) scaffold structure effectively reducing both the minimum volume and overflow of the precursor solution. We think this is because any excess perovskite then spills onto the part of the glass that is already in contact with the cell. With the active region of the cell above (uphill from) the back contact if we drop the perovskite precursor onto the active region, the solution fills out the active area of the cell without any overflow of perovskite past the ZrO₂ insulating layer yet continues down to create the back contact. After infiltration, we bake at 60°C for an hour and apply silver paint to facilitate robust contact points for our electrodes.

B. Imaging techniques

We use multiple forms of imaging for insight into our solar cells. First, we make images with a student-built Laser Beam Induced Current (LBIC) mapping system consisting of a 403nm laser $\sim 50 \mathrm{mW}$ scanner combined with a computer-controlled oscilloscope and data analysis software. Our system records a current reading for every point as the laser rasters over the cell, allowing us to make a spatial map of photocurrent generation. Areas in which the cell is performing poorly reveal spot defects and other fabrication or degradation problems: for example, our first cells had dark circles in the middle due non uniform layer thicknesses.

In addition to the LBIC, we can also take images of our cell using an optical microscope. The combination of images from the LBIC and optical microscope enhances our understanding of cell performance. A defect in an LBIC image often appears in the optical image as well (Figs. 3 and 4)—this is informative because we can accurately identify that a visible feature in the cell is likely to affect cell performance without looking at the LBIC first. This is valuable because visual inspection is rapid compared with LBIC mapping.

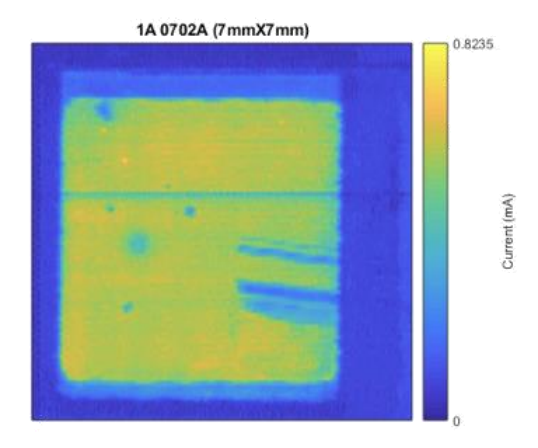


Fig. 3. This LBIC image contrasts areas of high performance (yellow), and low performance (blue), with a maximum current of 0.8235 mA. Only the active, electron-generating TiO2 layer is visible here, which is expected. There are a few spot defects due to dust, an accidental fingerprint on the right hand side, and a blue horizontal line due to an imaging software artifact

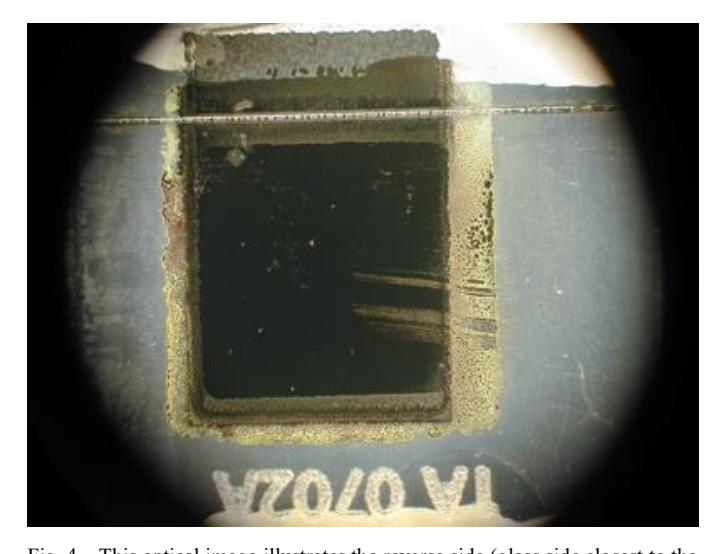


Fig. 4. This optical image illustrates the reverse side (glass side closest to the camera) of the same cell as Fig. 3, with the same orientation. The fingerprint is clearly shown in the same place, as well as a few spot defects due to dust.

C. Statistics



Fig. 5. Data output of cells automatically generated by Python

We use custom Python programs to automate data analysis, statistics, and visualization of batch processes. Each substrate has 36 cells fabricated in 6 x 6 grid. As shown in Fig. 5. After measuring all the cells, we can see the spatial pattern of the

performance of the key PV parameters extracted from the IV curves across our substrate. This helps us to understand an optimize the uniformity of our fabrication process. Color coding gives quick identification of each of the four quartiles of efficiency on a given substrate, and indicates if the performance was better in forward or reverse scans. The *IV* curve of the best cell on the substrate is plotted along with statistics for efficiency, fill factor, current density, and open circuit voltage.

III. RESULTS

In July 2019 we fabricated and tested 690 cells. 602 cells were viable with efficiency above 1%, an 87% yield. Our cells achieve peak efficiency after a few days, due to the slow crystallization of the perovskite, and stabilization of interfaces.

A. Indoor IV data

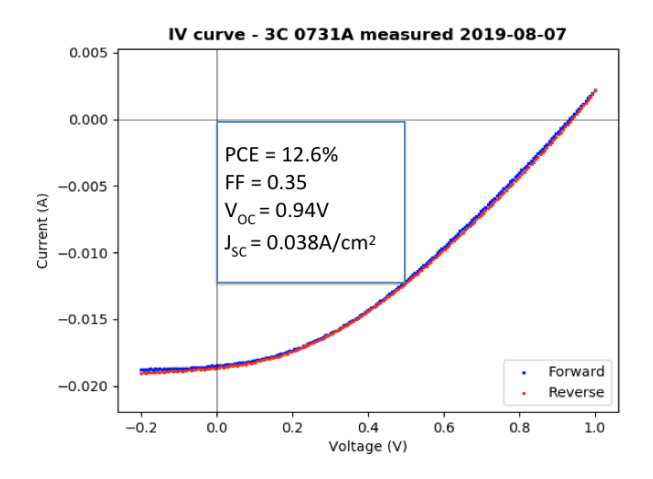
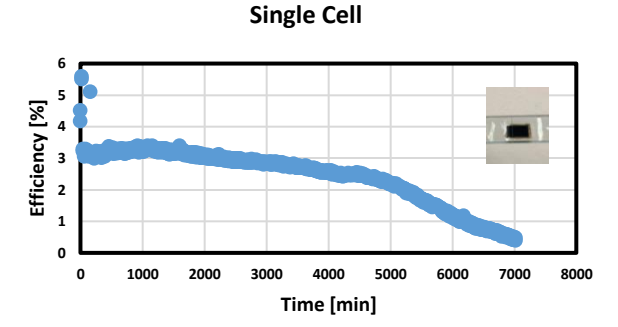


Fig. 6. IV measurement of our champion cell with efficiency 12.6%.

All of our *IV* data has been collected under a 500W LUXIM Light Emitting Plasma (LEP) lamp, which while not a calibrated certified solar simulator, has a spectrum similar to AM 1.5G, enabling cells to produce short circuit current densities above 30mA/cm², which is anomalously higher than anticipated, and a typical open circuit voltage up to 0.9V. We measure 1 sun power at the sample position with a thermal power meter (Thorlabs, S401C). In addition, our fill factors were around 0.35-0.4, which is clearly an area where we can expect to make improvements. To date our champion cell achieved an efficiency of 12.6%, with a short circuit current density of 38mA/cm² and an open circuit voltage of 0.94V, with a fill factor of 0.35 as shown in Fig. 6.

B. Stability data



Six Cell Module

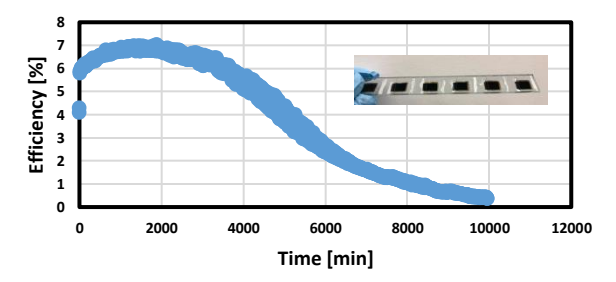


Fig. 7. Efficiency of a module of 6 solar cells under continuous illumination over time.

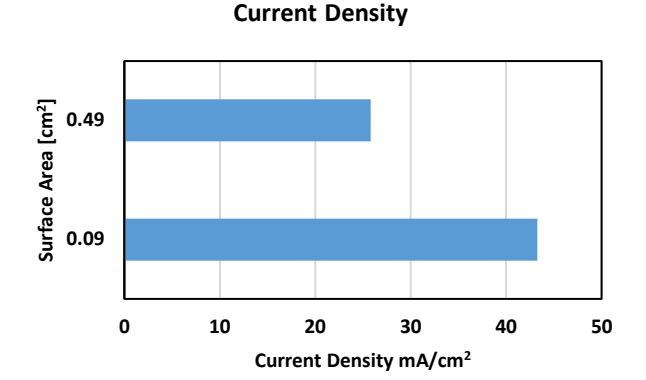
We observe that our devices are stable in dark dry storage for months. As a more challenging test of the stability we measured the performance of a module of 6 cells (0731A) connected in series over time under continuous illumination of the LEP lamp at an intensity of 100mW/cm². We took *IV* curve measurements of the module twice every 20 minutes, a forward sweeping measurement and a reverse sweeping measurement.

As seen in Fig. 7, our initial efficiency values were just over 4%. The jump in performance after the first measurement may indicate an "activation" of the module, after which we see a steady increase in efficiency until it peaks at 7% after 1900 minutes, or approximately 1.3 days of continuous irradiation.

After it peaks at 7%, we see a steep decline in efficiency until it falls below 1% efficiency after 8100 minutes, or approximately 5.6 days. At the end of the cycle we measured all 6 cells individually, and most of the cells were still operational except for one which seemed to become the weak link in the module.

We conducted the same experiment on a single cell. As in the case with the module, there was a jump in performance after the first measurement, supporting the "activation" phenomenon. We saw a steady increase in efficiency until it peaks above 3% after 0.8 days, followed by a steep decline until it falls below 1% efficiency after 6120 minutes, or 4.3 days.

IV. DISCUSSION



Open Circuit Voltage

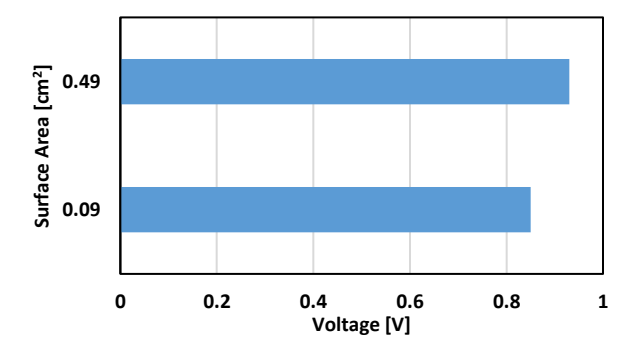


Fig. 8. Current density and open circuit voltage of the same cell with different illumination areas.



Fig. 9. Cell with carbon mask to reduce active area from $0.49~{\rm cm^2}$ to $0.09~{\rm cm^2}$.

As a method of investigating the effect of the active area of our cells, we conducted performance measurements of the same cell with an active area of 0.49 cm² and 0.09 cm². We saw that there was a sharp increase in current density from approximately 26 mA/cm² to over 40 mA/cm², suggesting that a larger active area is not uniformly efficient as the central region, and that there may be enhanced degradation, scattering, or traps near the edges of the cell. In contrast, we noticed that the change in open circuit voltage was much smaller.

We make 36 individual cells per substrate with our current screen-printing setup, but this maximum is limited mostly by the size of our printing stations and annealing hot plates. This implies that our fabrication design is easily scalable by simply increasing the size of our screen-printing system. Moreover, we are able to keep manufacturing costs low by using earthabundant carbon as our back-electrode material instead of gold and spiro-OMeTAD as the back electrode and hole transfer layer materials respectively, both of which are expensive materials in comparison to carbon. Our screen-printing setup is also conducive to experimenting with different layers or combinations of materials in our solar cells without needing to change much of the existing fabrication process. For example, if we want to use a different material for our electron transport layer, we can easily make that change by changing the ink composition. Our production capabilities make it easier to accumulate a significant data set of many cells of different designs for comparison.

We will continue to conduct cycling experiments to investigate the possibility of reversible and irreversible recovery of the cells, in addition to more controlled stability experiments in encapsulated or temperature-controlled environments. Moreover, we hope to reduce series resistance to improve our cell performance. We use an outdoor rooftop solar tracker and data acquisition instrumentation (also designed and built by undergraduate students) so that we can perform realistic lifetime studies in a true Southern California operating environment. Aging studies will be performed with intermittent interruptions to correlate changes in performance with evolution of LBIC maps and IPCE measurements. These approaches have been previously applied extensively to understand the degradation mechanisms of organic solar cells using protocols established at ISOS workshops [3] We will also reproduce data with other laboratories to corroborate our findings.

In summary, we demonstrated an effective method of scalable perovskite solar cell production by screen printing each layer of the cells in quick succession to make 36 viable solar cells in a single cycle. On a glass substrate, we screen printed a mesoporous layer of TiO2 as the electron transport layer, a mesoporous layer of ZrO₂ as the insulating layer, and a layer of carbon as the back electrode, with perovskite ink injected into the mesoporous layers to form a cell. Using this method, we fabricated and tested 690 cells, with our champion cell achieving a 12.6% efficiency, with a short circuit current density of 38 mA/cm² and an open circuit voltage of 0.94 V. We also tested the stability of a module of 6 solar cells under continuous illumination, and we noticed an initial increase of performance over 1.3 days, followed by a decline in performance until the efficiency fell below 1% after 5.6 days. To examine the presence and the effect of defects, we utilized a combination of LBIC imaging and optical imaging methods.

ACKNOWLEDGMENT

Our work benefits from extensive technical support and helpful interactions from both Trystan Watson's group at SPECIFIC in Swansea and the Monica Lira-Cantu's group at ICN2 in Barcelona.

REFERENCES

- [1] Y. Rong et al., "Beyond efficiency: the challenge of stability in mesoscopic perovskite solar cells," Adv. Energy Mater. 5(20), 2015 [doi:10.1002/aenm.201501066].
- [2] S. G. Hashmi et al., "Air processed inkjet infiltrated carbon based printed perovskite solar cells with high stability and reproducibility," Adv. Mater. Technol. 2(1), 2017 [doi:10.1002/admt.201600183].
- [3] D. M. Tanenbaum et al., "The ISOS-3 inter-laboratory collaboration focused on the stability of a variety of organic photovoltaic devices," Rsc Adv. 2(3), 882–893, 2012 [doi:10.1039/c1ra00686j].
- [4] F. De Rossi et al., "An interlaboratory study on the stability of all-printable hole transport material-free perovskite solar cells," Energy Technol., 2020 [doi: 10.1002/ente.202000134].
- [5] M. Hu et al., "Efficient hole-conductor-free, fully printable mesoscopic perovskite solar cells with a broad lightharvester NH2CH=NH2PbI3," J. Mater. Chem. A 2, 2014 [doi: 10.1039/C4TA03741C]